JACS
JOURNAL OF THE AMERICAN CHEMICAL SOCIETY
pubs.acs.org/JACS
Communication

Unveiling Charge-Pair Salt-Bridge Interaction Between GAGs and Collagen Protein in Cartilage: Atomic Evidence from DNP-Enhanced ssNMR at Natural Isotopic Abundance

Navneet Dwivedi,[‖] Bijaylaxmi Patra,[‖] Frederic Mentink-Vigier, Sungsool Wi,[*] and Neeraj Sinha[*]

Cite This: https://doi.org/10.1021/jacs.4c05539
Read Online

ABSTRACT: The interactions between glycosaminoglycans (GAGs) and proteins are essential in numerous biochemical processes that involve ion-pair interactions. However, there is no evidence of direct and specific interactions between GAGs and collagen proteins in native cartilage. The resolution of solid-state NMR (ssNMR) can offer such information but the detection of GAG interactions in cartilage is limited by the sensitivity of the experiments when ^{13}C and ^{15}N isotopes are at natural abundance. In this communication, this limitation is overcome by taking advantage of dynamic nuclear polarization (DNP)-enhanced magic-angle spinning (MAS) experiments to obtain two-dimensional (2D) $^{15}N-^{13}C$ and $^{13}C-^{13}C$ correlations on native samples at natural abundance. These experiments unveiled inter-residue correlations in the aliphatic regions of the collagen protein previously unobserved. Additionally, our findings provide direct evidence of charge−pair salt−bridge interactions between negatively charged GAGs and positively charged arginine (Arg) residues of collagen protein. We also identified potential hydrogen bonding interactions between hydroxyproline (Hyp) and GAGs, offering atomic insights into the biochemical interactions within the extracellular matrix of native cartilage. Our approach may provide a new avenue for the structural characterization of other native systems.

Supramolecular noncovalent interactions among molecules are crucial in various chemical and biological systems. They play important roles in the interaction of GAGs with a wide array of proteins including neutrophil-activating chemokines, fibroblast growth factors, and heparan sulfate−binding proteins.[1−3] This Communication presents direct evidence of probing these interactions in native cartilage, an area that has remained unexplored by biochemists until now. Cartilage is known to be a specialized connective tissue distributed throughout the body. It provides flexible and resilient support, cushions joints, facilitates movement, and absorbs shocks.[4−6] The extracellular matrix (ECM) of cartilage mainly comprises type II collagen protein (∼12% by weight), proteoglycan (∼6% by weight), water (∼82% by weight), and non-collagenous proteins, such as cartilage oligomeric matrix protein, matrilin-1, and cartilage intermediate-layer protein.[7−11] Proteoglycans further consist of proteins and polysaccharide chains, including chondroitin sulfate, keratan sulfate, heparan sulfate (HS), and hyaluronan, which are collectively known as GAGs.[12−14]

The cartilage ECM is a complex structure, characterized by highly mobile GAGs juxtaposed with rigid collagen proteins (Figure 1).[15,16] The interactions between proteins and GAGs are biologically critical as they regulate a diverse array of processes in the physiological system.[17−20] Interaction of GAGs, especially with collagen proteins, is essential for cartilage stability and despite its significance, studies on their nanoscale interaction at natural abundance are limited.[7,13,21−24] This current study confirms coulombic forces between the positively charged basic amino acids of proteins and the negatively charged anionic groups of GAGs.[25] The

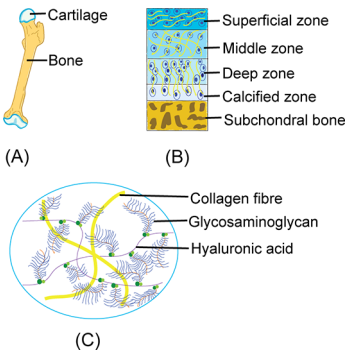

Figure 1. (A) Bone and cartilage. (B) Microstructure of cartilage. (C) Molecular view of cartilage ECM.

conventional models involve interactions between proteins and HS of GAGs that are predominantly governed by ion-pair interactions and are often termed salt bridges.[1,2,26−29] Despite this well-established concept, there is no direct evidence of this specific interaction in cartilage. One of the reasons for this knowledge gap can be the inherent molecular mobility of GAGs, which makes it very challenging for various techniques to study their interaction in the native state. To investigate

Received: April 23, 2024
Revised: July 3, 2024
Accepted: July 5, 2024

GAG−protein interactions,[30−33] solid-state NMR (ssNMR) spectroscopy has proved to be particularly valuable for elucidating local structures, dynamics, and interactions within cartilage on the molecular level.[34−40] This technique has also been used to study native collagen and extracted collagen,[41−43] but the understanding of their interactions with less abundant components in native cartilage ECM is challenging due to the inherent molecular mobility of GAGs. Indeed, the mobility and limited sensitivity of ssNMR at natural ^{13}C and ^{15}N isotopic abundance[7,38] make detecting these interactions difficult. The sensitivity of the experiment is usually addressed by isotopic labeling for NMR, which is a costly and challenging process for bones/cartilage.[34,44−46] To avoid the need for isotopic labeling, here we combined magic angle spinning dynamic nuclear polarization (MAS-DNP) enhancement with multidimensional ssNMR spectroscopy.[47−54] Carried out at low temperature, 100 K, this froze the motion of the GAGs and enabled the detection of weak NMR signals that cannot be observed using conventional MAS ssNMR methods alone. Importantly, the sample preparation is intended to maximize the sensitivity,[55] which enabled the recording of $^{15}N-^{13}C$ correlation experiments. The reported spectra herein represent a significant milestone: they are the first obtained on bones and cartilage at a natural isotopic abundance.

Finally, building upon previous investigations,[7,39,56−61] we achieved successful identification and assignment of the ^{13}C and ^{15}N resonances present in the organic matrices of bone and cartilage. Interestingly, we identified the interaction between GAGs and collagen in the assignment, which will be discussed below.

First, the DNP-enhanced cross-polarization (CP)MAS NMR spectra measured on the native bone and cartilage samples successfully facilitate the assignments of most of the ^{13}C and ^{15}N resonances from the organic matrix, with particular emphasis on the collagen protein containing glycine (Gly), proline (Pro), and hydroxyproline (Hyp). Remarkably, these ^{13}C resonances (Figure 2) exhibit similarities to spectra obtained via conventional ssNMR.[38,62−64] This similarity suggests that the sample preparation preserves the structural integrity of the organic matrix and is suitable for MAS DNP ssNMR studies.

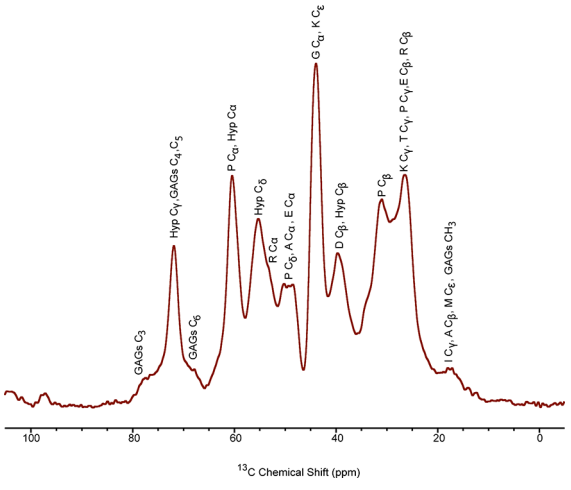

Figure 2. ^{13}C aliphatic resonances of the cartilage ECM at natural isotopic abundance. The one-letter codes for different amino acids are as follows: I for isoleucine, A for alanine, M for methionine, K for lysine, T for threonine, P for proline, E for glutamate, R for arginine, D for aspartate, Hyp for hydroxyproline, and G for glycine. Lists of chemical shifts are available in SI Table S7.

To obtain structural information, we employed 2D $^{15}N-^{13}C$ (NC) correlations and double-quantum filtered (DQF) single quantum (SQ)−single quantum (SQ) $^{13}C-^{13}C$ correlations.[57,65,66] We emphasize that acquiring the correlation spectra presented in Figure 3 represents a remarkable

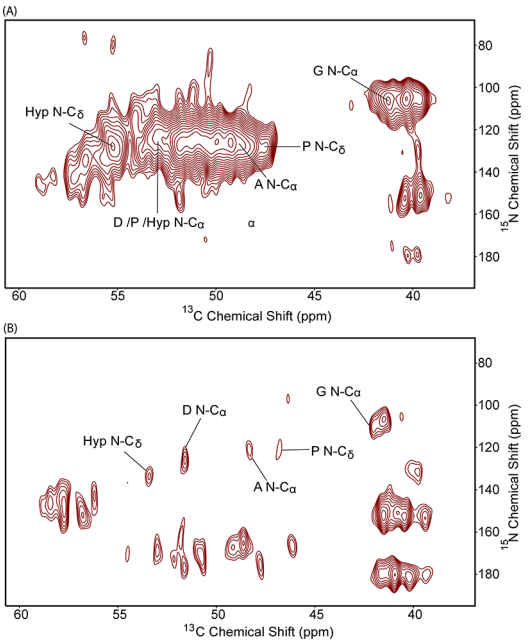

Figure 3. DNP-enhanced 2D $^{15}N-^{13}C$ dipolar correlation spectra of natural ^{15}N and ^{13}C abundance in cartilage (A) and bone (B). Full spectral region figures, lists of chemical shifts, S/N ratio, line width of assigned peaks, and amino acid distributions in COL1A1 and COL2A1 are provided in the SI.

achievement. The scarcity of ^{15}N (natural abundance: 0.37%), with its low gyromagnetic ratio (-2.71×10^7 rad T^{-1} s^{-1}), poses substantial challenges in detecting the ^{15}N spectra of collagen protein at its natural abundance using conventional ssNMR techniques. Combined with the low natural abundance of ^{13}C (1%) renders conventional ssNMR nearly impractical for generating a 2D $^{15}N-^{13}C$ correlation spectrum. The 2D $^{15}N-^{13}C$ correlation spectra, while common in biological NMR,[67,68] are rarely reported at natural isotopic abundance.[55,69−71] The experiments require a significant NMR sensitivity gain to begin with and thus require careful sample preparation. High sensitivity was obtained by DNP via the use of AsymPol-POK that enables the employment of a very short signal acquisition delay.[55,72] This biradical, used to enhance the NMR sensitivity with DNP, is particularly adapted to such conditions. In cartilage, it generated an enhancement of ∼85 for $^1H-^{13}C$ CPMAS and a short hyperpolarization time of ∼1.5 s, whereas in bone, it generates an enhancement of ∼50. In applying $^1H-^{15}N$ CPMAS to the same sample under these conditions, observation was not possible without microwave irradiation in a reasonable amount of time. However, the spectrum possesses an excellent S/N ratio under the microwave irradiation (see Figure S1 and Table S3 of the Supporting Information). Using DNP enhanced $^{15}N-^{13}C$ heteronuclear dipolar correlations, we explored the backbone

https://doi.org/10.1021/jacs.4c05539
J. Am. Chem. Soc. XXXX, XXX, XXX−XXX

structure of natural collagen protein within bone and cartilage matrices.

The 2D $^{15}N-^{13}C$ dipolar correlation spectra of cartilage and bone samples (Figures 3) show interesting differences in how collagen protein resonances are arranged in both spectra. The line width for signals of collagen in cartilage (SI Table S3) is broader in comparison to bone (SI Table S4). ProHypGly is known to be the most common triplet of collagen[73] and allows the tight packing and stability of triple helices. Indeed, we found their resonances in both the spectra with little variations in their chemical environment; e.g., Gly C_α (41.2 ppm) shows correlation with Gly N (106.6 ppm) in Figure 3A, whereas in Figure 3B, Gly C_α (42.1 ppm) shows correlation with Gly N at 109.7 ppm. Pro C_δ (47.5 ppm) shows correlation with Pro N at 128.8 ppm (Figure 3A), whereas in Figure 3B Pro C_δ (46.5 ppm) correlates with Pro N at 122.2 ppm. Hyp C_δ (55.1 ppm) shows correlation with Hyp N (128.1 ppm) in Figure 3A, whereas in the bone spectrum Hyp C_δ (53.4 ppm) shows correlation with Hyp N at 133.7 ppm. The difference of chemical shifts has also been seen in aliphatic amino acid alanine and negatively charged amino acid aspartate. Ala Cα (48.6 ppm) shows a cross-peak with Ala N at 127.1 ppm (Figure 3A), whereas in Figure 3B Ala Cα (48.3 ppm) shows a correlation with Ala N at 120.6 ppm. In the cartilage spectrum, Asp Cα (52.9 ppm) shows a cross-peak with Asp N at 123.7 ppm. This cross-peak, along with overlapped peaks of Pro Cα and Hyp Cα, produces a strong signal at ~52 ppm of the ^{13}C chemical shift. In contrast, the bone spectrum shows only the correlation of Asp Cα (51.5 ppm) with Asp N at 126.3 ppm. The unassigned signals detected between 140 and 180 ppm in the ^{15}N chemical shift are likely from DNA bases, since the sample may contain cells (e.g., chondrocytes, osteoblasts, osteoclasts, or osteocytes).[74] The observed differences between collagen resonances of type I in bone and collagen type II in cartilage may involve different levels of water accessibility for collagen in these tissues. This, in turn, could affect the DNP efficiency.

To further refine our model, we used DQF SQ–SQ $^{13}C-^{13}C$ experiments to probe the spatial proximities of ^{13}C. Whereas this experiment has similar sensitivity as compared to the conventional double quantum (DQ)–single quantum (SQ) INADEQUATE method,[45,65,75−77] the DQF SQ–SQ $^{13}C-^{13}C$ correlations offer advantages over the conventional DQ–SQ approach, notably an expanded measurable distance range by employing an extended mixing time which is not subject to pulse imperfections.[57] Here, the experiment employed a dipolar-assisted rotational recoupling (DARR) scheme,[78] with mixing times of 20 and 80 ms (Figure 4A and B, respectively). The DQF-DARR type experiment allows for the correlation of ^{13}C pairs separated up to a range of 4–5 Å.[79] Utilizing the identical sample preparation,[72] we obtained $^{13}C-^{13}C$ correlations between carbons of GAGs and collagen.

The aliphatic and carbonyl portions of the 2D $^{13}C-^{13}C$ dipolar correlation spectra of cartilage (Figure 4), obtained through the DQF-DARR mixing scheme. In this study, the majority of the detected ^{13}C signals in 2D $^{13}C-^{13}C$ cross-peaks originate from type II collagen. Proline (P) and hydroxyproline (Hyp) along with unique intra-residue correlations involving arginine (R) and glutamate (E) were observed in the aliphatic region (Figure 4A). Previous findings in the 2D $^{13}C-^{13}C$ dipolar correlation spectra of bone, using the DQF-DARR method with a 20 ms mixing time, revealed some intraresidue

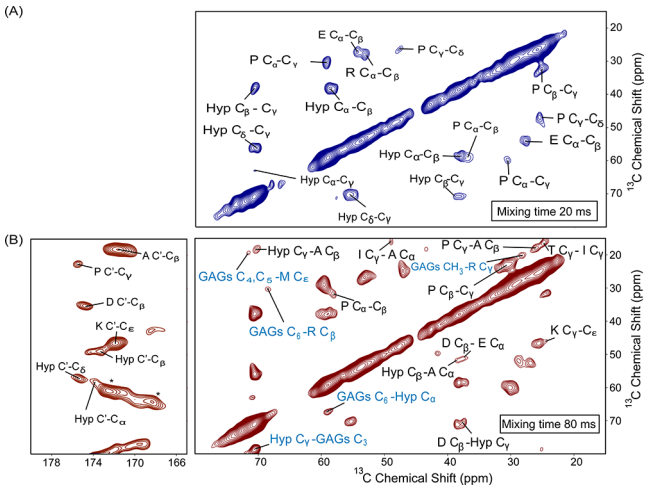

Figure 4. DQF 2D SQ–SQ $^{13}C-^{13}C$ dipolar correlation spectra of cartilage by using the DARR mixing scheme. To obtain $^{13}C-^{13}C$ correlations, two different DARR mixing times of 20 (Figure 4A) and 80 ms (Figure 4B) were used after a DQF block that is required to suppress dominant SQ ^{13}C coherences. The signals observed in the cross-peak regions of 168–174 ppm (F_2) and 60–80 ppm (F_1) are spinning-induced sidebands or artifacts that are denoted by asterisks (*). Full spectral region figures, an overlay figure, and a list of chemical shifts are available in the SI.

correlations in the carbonyl region.[57] However, when we repeated the same experiment with the same DARR mixing time on cartilage, no correlations were observed in the carbonyl region (Figure 4A).

To uncover the longer-range $^{13}C-^{13}C$ correlations, the DARR mixing time was extended to 80 ms, for which additional cross-peaks emerged. They reveal not only intra-residue correlations but also numerous inter-residue correlations in the aliphatic regions (Figure 4B). One remarkable aspect is the observation of signal enhancement in various ^{13}C resonances within the cartilage matrix (Figure S1). Notably, the GAG ring carbons, located at 20.2, 68.4, 71.5, and 78.7 ppm in Figure 4B, exhibited increased signal intensity. This enhancement is particularly intriguing given that GAGs are known to be less abundant components within the cartilage ECM.[7] Moreover, Figure 4B displays the presence of aliphatic isoleucine and methionine resonances along with charged aspartate and glutamate resonances. In the previous bone study, with a similar DARR mixing time, these resonances were invisible.[57] Interestingly, our current research revealed additional correlations between pyranose ring carbons and collagen. These are related to the intermolecular charge-pair salt-bridge-type interaction between the sulfate group of GAGs and Nε of the guanidinium group of Arg, along with N–H···O hydrogen bonding between the CO group of GAGs and NH^{2+} of the guanidinium group of Arg. These interactions facilitate the orientation of carbons, allowing them to be approximately 4–5 Å closer.[79] However, no anomeric carbon (C1)–collagen correlations were observed in the spectra. Notable $^{13}C-^{13}C$ dipolar correlations found in Figure 4B include (1) GAGs CH_3 (20.2 ppm) resonance with Arg Cγ (28.1 ppm), (2) GAGs C_6 (68.4 ppm) resonance with Arg C_β (30.3 ppm) and Hyp C_α (58.9 ppm), (3) GAGs C_4 and C_5 (71.5 ppm) resonance with Met C_ε (19.4 ppm), and (4) GAGs C_3 resonance at 78.7 ppm with Hyp C_γ (70.5 ppm). The correlation observed between the carbons of GAGs and Hyp arises from their spatial

https://doi.org/10.1021/jacs.4c05539
J. Am. Chem. Soc. XXXX, XXX, XXX–XXX

proximity, which resulted from O−H···O hydrogen bonding involving their hydroxyl groups.

Figure 5 is a 3D model-based visualization that we are observing as cross-peaks between GAGs and amino acids of collagen protein in the 2D $^{13}C-^{13}C$ spectra (Figure 4B). The correlations observed in Figure 4B highlight the spatial association between GAG carbons and collagen residues. This spatial relationship is established through $^{13}C-^{13}C$ dipolar coupling networks that resulted from the charge-pair salt-bridge interaction between negatively charged GAGs and positively charged Arg residues and hydrogen bonding between GAGs and Hyp of collagen protein within the cartilage ECM. These findings confirm the existence of these specific types of interactions in cartilage ECM, which had no direct atomic level evidence previously. The results not only unveil atomic insights about the intricate biochemical interaction within native cartilage ECM but are also paving a way for exciting new possibilities in exploring structural intricacies of other native systems.

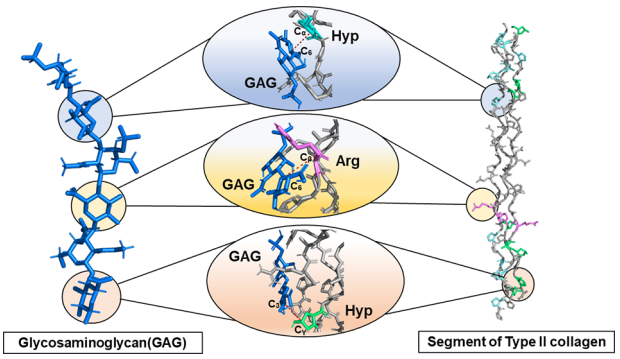

Figure 5. 3D model showing interaction between glycosaminoglycan (PDB ID: 1C4S) and a segment of type II collagen (PDB ID: 6JEC). Distances of the observed restraints are available in the Supporting Information, Table S9.

■ ASSOCIATED CONTENT

Supporting Information

The Supporting Information is available free of charge at https://pubs.acs.org/doi/10.1021/jacs.4c05539.

Experimental details; 1D $^{1}H-^{15}N$ CPMAS; $^{1}H-^{13}C$ CPMAS spectra of bone and cartilage; full region spectra of 2D $^{15}N-^{13}C$ correlation spectra and 2D DQF-DARR $^{13}C-^{13}C$ correlation spectra along with their overlay spectra; 3D models of the interactions between GAGs and collagen; and the tables of amino acid distribution, S/N ratio, line widths of 2D $^{15}N-^{13}C$ correlation spectra, chemical shifts of the assigned peaks, and distances of the restraints observed in the docked model; and supplementary references (PDF)

■ AUTHOR INFORMATION

Corresponding Authors

Neeraj Sinha − *Centre of Biomedical Research, Lucknow 226014, India; Academy of Scientific and Innovative Research (AcSIR), Ghaziabad 201002, India;* orcid.org/0000-0003-3235-6127; Email: neerajcbmr@gmail.com, neeraj.sinha@cbmr.res.in

Sungsool Wi − *National High Magnetic Field Laboratory, Florida State University, Tallahassee, Florida 32310, United States*; Email: sungsool@magnet.fsu.edu

Authors

Navneet Dwivedi − *Centre of Biomedical Research, Lucknow 226014, India*

Bijaylaxmi Patra − *Centre of Biomedical Research, Lucknow 226014, India; Academy of Scientific and Innovative Research (AcSIR), Ghaziabad 201002, India*

Frederic Mentink-Vigier − *National High Magnetic Field Laboratory, Florida State University, Tallahassee, Florida 32310, United States;* orcid.org/0000-0002-3570-9787

Complete contact information is available at: https://pubs.acs.org/10.1021/jacs.4c05539

Author Contributions

‖These authors contributed equally.

Notes

The authors declare no competing financial interest.

■ ACKNOWLEDGMENTS

Partial support for this research was provided by the National High Magnetic Field Laboratory, funded through the National Science Foundation under Cooperative Agreement Nos. DMR-1644779 and DMR-2128556, as well as support from the state of Florida. The MAS-DNP instrument is supported by NIH P41 GM122698 and NIH RM1-GM148766. B.P. acknowledges AcSIR (Academy of Scientific and Innovative Research) for the registration (Registration No. 10BB22A71003) and is thankful for financial assistance from the University Grants Commission (UGC). We also acknowledge Mr. Ali Kausar for his assistance in designing the cover art.

■ REFERENCES

(1) Joseph, P. R. B.; Sawant, K. V.; Iwahara, J.; Garofalo, R. P.; Desai, U. R.; Rajarathnam, K. Lysines and Arginines Play Non-Redundant Roles in Mediating Chemokine-Glycosaminoglycan Interactions. *Sci. Rep.* **2018**, *8* (1), 12289.

(2) Fromm, J. R.; Hileman, R. E.; Weiler, J. M.; Linhardt, R. J. Interaction of Fibroblast Growth Factor-1 and Related Peptides with Heparan Sulfate and Its Oligosaccharides. *Arch. Biochem. Biophys.* **1997**, *346* (2), 252−262.

(3) Xu, D.; Esko, J. D. Demystifying Heparan Sulfate-Protein Interactions. *Annu. Rev. Biochem.* **2014**, *83*, 129−157.

(4) Sophia Fox, A. J.; Bedi, A.; Rodeo, S. A. The Basic Science of Articular Cartilage: Structure, Composition, and Function. *Sports Health* **2009**, *1* (6), 461−468.

(5) Abe, K.; Yamashita, A.; Morioka, M.; Horike, N.; Takei, Y.; Koyamatsu, S.; Okita, K.; Matsuda, S.; Tsumaki, N. Engraftment of Allogeneic iPS Cell-Derived Cartilage Organoid in a Primate Model of Articular Cartilage Defect. *Nat. Commun.* **2023**, *14* (1), 804.

(6) Han, L.; Grodzinsky, A. J.; Ortiz, C. Nanomechanics of the Cartilage Extracellular Matrix. *Annu. Rev. Mater. Res.* **2011**, *41*, 133−168.

(7) Tiwari, N.; Wi, S.; Mentink-Vigier, F.; Sinha, N. Mechanistic Insights into the Structural Stability of Collagen-Containing Biomaterials Such as Bones and Cartilage. *J. Phys. Chem. B* **2021**, *125* (18), 4757−4766.

(8) Hunter, C. J.; Mouw, J. K.; Levenston, M. E. Dynamic Compression of Chondrocyte-Seeded Fibrin Gels: Effects on Matrix Accumulation and Mechanical Stiffness. *Osteoarthritis Cartilage* **2004**, *12* (2), 117−130.

(9) van den Boom, R.; Brama, P. A. J.; Kiers, G. H.; de Groot, J.; van Weeren, P. R. Assessment of the Effects of Age and Joint Disease on Hydroxyproline and Glycosaminoglycan Concentrations in Synovial Fluid from the Metacarpophalangeal Joint of Horses. *Am. J. Vet. Res.* **2004**, *65* (3), 296−302.
(10) Fragonas, E.; Mlynárik, V.; Jellús, V.; Micali, F.; Piras, A.; Toffanin, R.; Rizzo, R.; Vittur, F. Correlation between Biochemical Composition and Magnetic Resonance Appearance of Articular Cartilage. *Osteoarthritis Cartilage* **1998**, *6* (1), 24−32.
(11) Krishnan, Y.; Grodzinsky, A. J. Cartilage Diseases. *Matrix Biol. J. Int. Soc. Matrix Biol.* **2018**, *71*−*72*, 51−69.
(12) Poole, A. R. Proteoglycans in Health and Disease: Structures and Functions. *Biochem. J.* **1986**, *236* (1), 1−14.
(13) Ng, L.; Grodzinsky, A. J.; Patwari, P.; Sandy, J.; Plaas, A.; Ortiz, C. Individual Cartilage Aggrecan Macromolecules and Their Constituent Glycosaminoglycans Visualized via Atomic Force Microscopy. *J. Struct. Biol.* **2003**, *143* (3), 242−257.
(14) Neves, M. I.; Araújo, M.; Moroni, L.; da Silva, R. M. P.; Barrias, C. C. Glycosaminoglycan-Inspired Biomaterials for the Development of Bioactive Hydrogel Networks. *Molecules* **2020**, *25* (4), DOI: 10.3390/molecules25040978.
(15) Acharya, C.; Yik, J. H. N.; Kishore, A.; Van Dinh, V.; Di Cesare, P. E.; Haudenschild, D. R. Cartilage Oligomeric Matrix Protein and Its Binding Partners in the Cartilage Extracellular Matrix: Interaction, Regulation and Role in Chondrogenesis. *Matrix Biol.* **2014**, *37*, 102−111.
(16) Asanbaeva, A.; Masuda, K.; Thonar, E. J.-M. A.; Klisch, S. M.; Sah, R. L. Mechanisms of Cartilage Growth: Modulation of Balance between Proteoglycan and Collagen in Vitro Using Chondroitinase ABC. *Arthritis Rheum.* **2007**, *56* (1), 188−198.
(17) Cardin, A. D.; Weintraub, H. J. Molecular Modeling of Protein-Glycosaminoglycan Interactions. *Arterioscler. Dallas Tex* **1989**, *9* (1), 21−32.
(18) Gandhi, N. S.; Mancera, R. L. The Structure of Glycosaminoglycans and Their Interactions with Proteins. *Chem. Biol. Drug Des.* **2008**, *72* (6), 455−482.
(19) Monneau, Y.; Arenzana-Seisdedos, F.; Lortat-Jacob, H. The Sweet Spot: How GAGs Help Chemokines Guide Migrating Cells. *J. Leukoc. Biol.* **2016**, *99* (6), 935−953.
(20) Raspanti, M.; Viola, M.; Forlino, A.; Tenni, R.; Gruppi, C.; Tira, M. E. Glycosaminoglycans Show a Specific Periodic Interaction with Type I Collagen Fibrils. *J. Struct. Biol.* **2008**, *164* (1), 134−139.
(21) Munakata, H.; Takagaki, K.; Majima, M.; Endo, M. Interaction between Collagens and Glycosaminoglycans Investigated Using a Surface Plasmon Resonance Biosensor. *Glycobiology* **1999**, *9* (10), 1023−1027.
(22) Roughley, P. J.; Lee, E. R. Cartilage Proteoglycans: Structure and Potential Functions. *Microsc. Res. Technol.* **1994**, *28* (5), 385−397.
(23) Aigner, T.; Stöve, J. Collagens—Major Component of the Physiological Cartilage Matrix, Major Target of Cartilage Degeneration, Major Tool in Cartilage Repair. *Adv. Drug Delivery Rev.* **2003**, *55* (12), 1569−1593.
(24) Roughley, P. J.; Mort, J. S. The Role of Aggrecan in Normal and Osteoarthritic Cartilage. *J. Exp. Orthop.* **2014**, *1* (1), 8.
(25) Fromm, J. R.; Hileman, R. E.; Caldwell, E. E.; Weiler, J. M.; Linhardt, R. J. Differences in the Interaction of Heparin with Arginine and Lysine and the Importance of These Basic Amino Acids in the Binding of Heparin to Acidic Fibroblast Growth Factor. *Arch. Biochem. Biophys.* **1995**, *323* (2), 279−287.
(26) Fromm, J. R.; Hileman, R. E.; Caldwell, E. E.; Weiler, J. M.; Linhardt, R. J. Pattern and Spacing of Basic Amino Acids in Heparin Binding Sites. *Arch. Biochem. Biophys.* **1997**, *343* (1), 92−100.
(27) Musafia, B.; Buchner, V.; Arad, D. Complex Salt Bridges in Proteins: Statistical Analysis of Structure and Function. *J. Mol. Biol.* **1995**, *254* (4), 761−770.
(28) Donald, J. E.; Kulp, D. W.; DeGrado, W. F. Salt Bridges: Geometrically Specific, Designable Interactions. *Proteins* **2011**, *79* (3), 898−915.
(29) Fallas, J. A.; Dong, J.; Tao, Y. J.; Hartgerink, J. D. Structural Insights into Charge Pair Interactions in Triple Helical Collagen-like Proteins. *J. Biol. Chem.* **2012**, *287* (11), 8039−8047.
(30) Künze, G.; Huster, D.; Samsonov, S. A. Investigation of the Structure of Regulatory Proteins Interacting with Glycosaminoglycans by Combining NMR Spectroscopy and Molecular Modeling - the Beginning of a Wonderful Friendship. *Biol. Chem.* **2021**, *402* (11), 1337−1355.
(31) Powell, A. K.; Yates, E. A.; Fernig, D. G.; Turnbull, J. E. Interactions of Heparin/Heparan Sulfate with Proteins: Appraisal of Structural Factors and Experimental Approaches. *Glycobiology* **2004**, *14* (4), 17R−30R.
(32) Perez, S.; Makshakova, O.; Angulo, J.; Bedini, E.; Bisio, A.; de Paz, J. L.; Fadda, E.; Guerrini, M.; Hricovini, M.; Hricovini, M.; Lisacek, F.; Nieto, P. M.; Pagel, K.; Paiardi, G.; Richter, R.; Samsonov, S. A.; Vivès, R. R.; Nikitovic, D.; Ricard Blum, S. Glycosaminoglycans: What Remains To Be Deciphered? *JACS Au* **2023**, *3* (3), 628−656.
(33) Chung, K.; Kim, J.; Cho, B.-K.; Ko, B.-J.; Hwang, B.-Y.; Kim, B.-G. How Does Dextran Sulfate Prevent Heat Induced Aggregation of Protein? The Mechanism and Its Limitation as Aggregation Inhibitor. *Biochim. Biophys. Acta* **2007**, *1774* (2), 249−257.
(34) Murgoci, A.; Duer, M. Molecular Conformations and Dynamics in the Extracellular Matrix of Mammalian Structural Tissues: Solid-State NMR Spectroscopy Approaches. *Matrix Biol. Plus* **2021**, *12*, No. 100086.
(35) Huster, D.; Naji, L.; Schiller, J.; Arnold, K. Dynamics of the Biopolymers in Articular Cartilage Studied by Magic Angle Spinning NMR. *Appl. Magn. Reson.* **2004**, *27* (3), 471−487.
(36) Scheidt, H. A.; Schibur, S.; Magalhães, A.; de Azevedo, E. R.; Bonagamba, T. J.; Pascui, O.; Schulz, R.; Reichert, D.; Huster, D. The Mobility of Chondroitin Sulfate in Articular and Artificial Cartilage Characterized by 13C Magic-Angle Spinning NMR Spectroscopy. *Biopolymers* **2010**, *93* (6), 520−532.
(37) Zernia, G.; Huster, D. Collagen Dynamics in Articular Cartilage under Osmotic Pressure. *NMR Biomed.* **2006**, *19* (8), 1010−1019.
(38) Naji, L.; Kaufmann, J.; Huster, D.; Schiller, J.; Arnold, K. 13C NMR Relaxation Studies on Cartilage and Cartilage Components. *Carbohydr. Res.* **2000**, *327* (4), 439−446.
(39) Xu, J.; Zhu, P.; Morris, M. D.; Ramamoorthy, A. Solid-State NMR Spectroscopy Provides Atomic-Level Insights Into the Dehydration of Cartilage. *J. Phys. Chem. B* **2011**, *115* (33), 9948−9954.
(40) Chow, W. Y.; Norman, B. P.; Roberts, N. B.; Ranganath, L. R.; Teutloff, C.; Bittl, R.; Duer, M. J.; Gallagher, J. A.; Oschkinat, H. Pigmentation Chemistry and Radical-Based Collagen Degradation in Alkaptonuria and Osteoarthritic Cartilage. *Angew. Chem., Int. Ed.* **2020**, *59* (29), 11937−11942.
(41) Mroue, K. H.; Viswan, A.; Sinha, N.; Ramamoorthy, A. Chapter Six - Solid-State NMR Spectroscopy: The Magic Wand to View Bone at Nanoscopic Resolution. In *Annu. Rep. NMR Spectrosc.*; Webb, G. A., Ed.; Academic Press, 2017; Vol. *92*, pp 365−413. DOI: 10.1016/bs.arnmr.2017.04.004.
(42) Rai, R. K.; Sinha, N. Dehydration-Induced Structural Changes in the Collagen−Hydroxyapatite Interface in Bone by High-Resolution Solid-State NMR Spectroscopy. *J. Phys. Chem. C* **2011**, *115* (29), 14219−14227.
(43) Goldberga, I.; Li, R.; Duer, M. J. Collagen Structure-Function Relationships from Solid-State NMR Spectroscopy. *Acc. Chem. Res.* **2018**, *51* (7), 1621−1629.
(44) Wong, V. W. C.; Reid, D. G.; Chow, W. Y.; Rajan, R.; Green, M.; Brooks, R. A.; Duer, M. J. Preparation of Highly and Generally Enriched Mammalian Tissues for Solid State NMR. *J. Biomol. NMR* **2015**, *63* (2), 119−123.
(45) Goldberga, I.; Li, R.; Ying Chow, W.; G. Reid, D.; Bashtanova, U.; Rajan, R.; Puszkarska, A.; Oschkinat, H.; J. Duer, M. Detection of Nucleic Acids and Other Low Abundance Components in Native Bone and Osteosarcoma Extracellular Matrix by Isotope Enrichment and DNP-Enhanced NMR. *RSC Adv.* **2019**, *9* (46), 26686−26690.

https://doi.org/10.1021/jacs.4c05539
J. Am. Chem. Soc. XXXX, XXX, XXX−XXX

(46) Duer, M. J. The Contribution of Solid-State NMR Spectroscopy to Understanding Biomineralization: Atomic and Molecular Structure of Bone. *J. Magn. Reson. San Diego Calif 1997* **2015**, *253*, 98−110.
(47) Lilly Thankamony, A. S.; Wittmann, J. J.; Kaushik, M.; Corzilius, B. Dynamic Nuclear Polarization for Sensitivity Enhancement in Modern Solid-State NMR. *Prog. Nucl. Magn. Reson. Spectrosc.* **2017**, *102*−*103*, 120−195.
(48) Rossini, A. J.; Widdifield, C. M.; Zagdoun, A.; Lelli, M.; Schwarzwälder, M.; Copéret, C.; Lesage, A.; Emsley, L. Dynamic Nuclear Polarization Enhanced NMR Spectroscopy for Pharmaceutical Formulations. *J. Am. Chem. Soc.* **2014**, *136* (6), 2324−2334.
(49) Cai, X.; Lucini Paioni, A.; Adler, A.; Yao, R.; Zhang, W.; Beriashvili, D.; Safeer, A.; Gurinov, A.; Rockenbauer, A.; Song, Y.; Baldus, M.; Liu, Y. Highly Efficient Trityl-Nitroxide Biradicals for Biomolecular High-Field Dynamic Nuclear Polarization. *Chem. − Eur. J.* **2021**, *27* (50), 12758−12762.
(50) Maly, T.; Debelouchina, G. T.; Bajaj, V. S.; Hu, K.-N.; Joo, C.-G.; Mak−Jurkauskas, M. L.; Sirigiri, J. R.; van der Wel, P. C. A.; Herzfeld, J.; Temkin, R. J.; Griffin, R. G. Dynamic Nuclear Polarization at High Magnetic Fields. *J. Chem. Phys.* **2008**, *128* (5), No. 052211.
(51) Jaudzems, K.; Polenova, T.; Pintacuda, G.; Oschkinat, H.; Lesage, A. DNP NMR of Biomolecular Assemblies. *J. Struct. Biol.* **2019**, *206* (1), 90−98.
(52) Biedenbänder, T.; Aladin, V.; Saeidpour, S.; Corzilius, B. Dynamic Nuclear Polarization for Sensitivity Enhancement in Biomolecular Solid-State NMR. *Chem. Rev.* **2022**, *122* (10), 9738−9794.
(53) Chow, W. Y.; De Paëpe, G.; Hediger, S. Biomolecular and Biological Applications of Solid-State NMR with Dynamic Nuclear Polarization Enhancement. *Chem. Rev.* **2022**, *122* (10), 9795−9847.
(54) Ghassemi, N.; Poulhazan, A.; Deligey, F.; Mentink-Vigier, F.; Marcotte, I.; Wang, T. Solid-State NMR Investigations of Extracellular Matrixes and Cell Walls of Algae, Bacteria, Fungi, and Plants. *Chem. Rev.* **2022**, *122* (10), 10036−10086.
(55) Harrabi, R.; Halbritter, T.; Aussenac, F.; Dakhlaoui, O.; van Tol, J.; Damodaran, K. K.; Lee, D.; Paul, S.; Hediger, S.; Mentink-Vigier, F.; Sigurdsson, S. Th.; De Paëpe, G. Highly Efficient Polarizing Agents for MAS-DNP of Proton-Dense Molecular Solids. *Angew. Chem., Int. Ed.* **2022**, *61* (12), No. e202114103.
(56) Rai, R. K.; Singh, C.; Sinha, N. Predominant Role of Water in Native Collagen Assembly inside the Bone Matrix. *J. Phys. Chem. B* **2015**, *119* (1), 201−211.
(57) Wi, S.; Dwivedi, N.; Dubey, R.; Mentink-Vigier, F.; Sinha, N. Dynamic Nuclear Polarization-Enhanced, Double-Quantum Filtered 13C-13C Dipolar Correlation Spectroscopy of Natural 13C Abundant Bone-Tissue Biomaterial. *J. Magn. Reson.* **2022**, *335*, No. 107144.
(58) Singh, C.; Rai, R. K.; Sinha, N. Experimental Aspect of Solid-State Nuclear Magnetic Resonance Studies of Biomaterials Such as Bones. *Solid State Nucl. Magn. Reson.* **2013**, *54*, 18−25.
(59) Chow, W. Y.; Rajan, R.; Muller, K. H.; Reid, D. G.; Skepper, J. N.; Wong, W. C.; Brooks, R. A.; Green, M.; Bihan, D.; Farndale, R. W.; Slatter, D. A.; Shanahan, C. M.; Duer, M. J. NMR Spectroscopy of Native and in Vitro Tissues Implicates polyADP Ribose in Biomineralization. *Science* **2014**, *344* (6185), 742−746.
(60) Pomin, V. H. NMR Chemical Shifts in Structural Biology of Glycosaminoglycans. *Anal. Chem.* **2014**, *86* (1), 65−94.
(61) Wise, E. R.; Maltsev, S.; Davies, M. E.; Duer, M. J.; Jaeger, C.; Loveridge, N.; Murray, R. C.; Reid, D. G. The Organic−Mineral Interface in Bone Is Predominantly Polysaccharide. *Chem. Mater.* **2007**, *19* (21), 5055−5057.
(62) Zhu, P.; Xu, J.; Sahar, N.; Morris, M. D.; Kohn, D. H.; Ramamoorthy, A. Time-Resolved Dehydration-Induced Structural Changes in an Intact Bovine Cortical Bone Revealed by Solid-State NMR Spectroscopy. *J. Am. Chem. Soc.* **2009**, *131* (47), 17064−17065.
(63) Duer, M. J.; Friščić, T.; Murray, R. C.; Reid, D. G.; Wise, E. R. The Mineral Phase of Calcified Cartilage: Its Molecular Structure and Interface with the Organic Matrix. *Biophys. J.* **2009**, *96* (8), 3372−3378.
(64) Viswan, A.; Sinha, N. Native Collagen and Its Structural Fulcrum through a Site Specific Hydration Topology Map. *J. Phys. Chem. C* **2017**, *121* (34), 18807−18814.
(65) Fernando, L. D.; Dickwella Widanage, M. C.; Shekar, S. C.; Mentink-Vigier, F.; Wang, P.; Wi, S.; Wang, T. Solid-State NMR Analysis of Unlabeled Fungal Cell Walls from *Aspergillus* and *Candida* Species. *J. Struct. Biol. X* **2022**, *6*, No. 100070.
(66) Wang, T.; Hong, M. Solid-State NMR Investigations of Cellulose Structure and Interactions with Matrix Polysaccharides in Plant Primary Cell Walls. *J. Exp. Bot.* **2016**, *67* (2), 503−514.
(67) De Paëpe, G.; Lewandowski, J.; Loquet, A.; Eddy, M.; Megy, S.; Böckmann, A.; Griffin, R. Heteronuclear Proton Assisted Recoupling. *J. Chem. Phys.* **2011**, *134*, No. 095101.
(68) Gelenter, M. D.; Hong, M. Efficient 15N-13C Polarization Transfer by Third-Spin Assisted Pulsed Cross Polarization Magic-Angle-Spinning NMR for Protein Structure Determination. *J. Phys. Chem. B* **2018**, *122* (35), 8367−8379.
(69) Märker, K.; Pingret, M.; Mouesca, J.-M.; Gasparutto, D.; Hediger, S.; De Paëpe, G. A New Tool for NMR Crystallography: Complete 13C/15N Assignment of Organic Molecules at Natural Isotopic Abundance Using DNP-Enhanced Solid-State NMR. *J. Am. Chem. Soc.* **2015**, *137* (43), 13796−13799.
(70) Smith, A. N.; Märker, K.; Hediger, S.; De Paëpe, G. Natural Isotopic Abundance 13C and 15N Multidimensional Solid-State NMR Enabled by Dynamic Nuclear Polarization. *J. Phys. Chem. Lett.* **2019**, *10* (16), 4652−4662.
(71) Jaroniec, C. P.; Tounge, B. A.; Herzfeld, J.; Griffin, R. G. Frequency Selective Heteronuclear Dipolar Recoupling in Rotating Solids: Accurate 13C−15N Distance Measurements in Uniformly 13C,15N-Labeled Peptides. *J. Am. Chem. Soc.* **2001**, *123* (15), 3507−3519.
(72) Mentink-Vigier, F.; Marin-Montesinos, I.; Jagtap, A. P.; Halbritter, T.; van Tol, J.; Hediger, S.; Lee, D.; Sigurdsson, S. Th.; De Paëpe, G. Computationally Assisted Design of Polarizing Agents for Dynamic Nuclear Polarization Enhanced NMR: The AsymPol Family. *J. Am. Chem. Soc.* **2018**, *140* (35), 11013−11019.
(73) Shoulders, M. D.; Raines, R. T. Collagen Structure and Stability. *Annu. Rev. Biochem.* **2009**, *78*, 929−958.
(74) Conroy, D. W.; Xu, Y.; Shi, H.; Gonzalez Salguero, N.; Purusottam, R. N.; Shannon, M. D.; Al-Hashimi, H. M.; Jaroniec, C. P. Probing Watson-Crick and Hoogsteen Base Pairing in Duplex DNA Using Dynamic Nuclear Polarization Solid-State NMR Spectroscopy. *Proc. Natl. Acad. Sci. U. S. A.* **2022**, *119* (30), No. e2200681119.
(75) Takahashi, H.; Lee, D.; Dubois, L.; Bardet, M.; Hediger, S.; De Paëpe, G. Rapid Natural-Abundance 2D 13C−13C Correlation Spectroscopy Using Dynamic Nuclear Polarization Enhanced Solid-State NMR and Matrix-Free Sample Preparation. *Angew. Chem., Int. Ed.* **2012**, *51* (47), 11766−11769.
(76) Rossini, A. J.; Zagdoun, A.; Hegner, F.; Schwarzwälder, M.; Gajan, D.; Copéret, C.; Lesage, A.; Emsley, L. Dynamic Nuclear Polarization NMR Spectroscopy of Microcrystalline Solids. *J. Am. Chem. Soc.* **2012**, *134* (40), 16899−16908.
(77) Najdanova, M.; Gräsing, D.; Alia, A.; Matysik, J. Analysis of the Electronic Structure of the Special Pair of a Bacterial Photosynthetic Reaction Center by 13C Photochemically Induced Dynamic Nuclear Polarization Magic-Angle Spinning NMR Using a Double-Quantum Axis. *Photochem. Photobiol.* **2018**, *94* (1), 69−80.
(78) Takegoshi, K.; Shinji, N.; Terao, T. $^{13}C-^{1}H$ Dipolar-Assisted Rotational Resonance in Magic-Angle Spinning NMR. *Chem. Phys. Lett.* **2001**, *344*, 631−637.
(79) Zhao, W.; Fernando, L. D.; Kirui, A.; Deligey, F.; Wang, T. Solid-State NMR of Plant and Fungal Cell Walls: A Critical Review. *Solid State Nucl. Magn. Reson.* **2020**, *107*, No. 101660.

https://doi.org/10.1021/jacs.4c05539
J. Am. Chem. Soc. XXXX, XXX, XXX−XXX